

This document was prepared in conjunction with work accomplished under Contract No. DE-AC09-96SR18500 with the U. S. Department of Energy.

DISCLAIMER

This report was prepared as an account of work sponsored by an agency of the United States Government. Neither the United States Government nor any agency thereof, nor any of their employees, nor any of their contractors, subcontractors or their employees, makes any warranty, express or implied, or assumes any legal liability or responsibility for the accuracy, completeness, or any third party's use or the results of such use of any information, apparatus, product, or process disclosed, or represents that its use would not infringe privately owned rights. Reference herein to any specific commercial product, process, or service by trade name, trademark, manufacturer, or otherwise, does not necessarily constitute or imply its endorsement, recommendation, or favoring by the United States Government or any agency thereof or its contractors or subcontractors. The views and opinions of authors expressed herein do not necessarily state or reflect those of the United States Government or any agency thereof.

A Transient Model of Induced Natural Circulation Thermal Cycling for Hydrogen Isotope Separation

Martin A. Shadday Jr. and Leung Kit Heung

Savannah River National Laboratory, Aiken, SC, USA, 29808,

martin.shadday@srnl.doe.gov

Abstract

The property of selective temperature dependence of adsorption and desorption of hydrogen isotopes by palladium is used for isotope separation. A proposal to use natural circulation of nitrogen to alternately heat and cool a packed bed of palladium coated beads is under active investigation, and a device consisting of two interlocking natural convection loops is being designed. A transient numerical model of the device has been developed to aid the design process. It is a one-dimensional finite-difference model, using the Boussinesq approximation. The thermal inertia of the pipe walls and other heat structures as well as the heater control logic is included in the model. Two system configurations were modelled and results are compared.

Nomenclature

A_f	section inlet/outlet area	Nu	Nusselt number
\bar{A}	section average flow area	P	pressure
A_s	heat transfer surface area	Pr	Prandtl number
C_p	solid heat structure specific heat	\dot{Q}	heat transfer rate
D	hydraulic diameter	Re	Reynolds number
\bar{F}	force	T	temperature
f	friction factor	t	time
g	gravitational acceleration	\bar{V}	velocity
h	convection heat transfer coefficient	V	volume
K	form loss coefficient	α	heater exponential constant
k	thermal conductivity	β	coefficient of thermal expansion
L	length	ρ	density
m	mass	μ	dynamic viscosity
\dot{m}	mass flowrate		

Introduction

The property of selective temperature dependence of adsorption and desorption of hydrogen isotopes by palladium is used for isotope separation. A proposal to use natural circulation of nitrogen to alternately heat and cool a packed bed of palladium coated beads is under active investigation. The packed bed is in a finned coil that is alternately heated and cooled between the temperature limits of -40 °C and 150 °C by the external flow of nitrogen. This design concept does not require pumps or compressors to circulate the heating and cooling fluid. A numerical model of the transient behavior of the two natural circulation loops or thermosyphons was developed to aid the design process. The model predicts the transient temperature of the palladium coated beads in the coil. The model is described and results are presented and discussed herein.

Two loop configurations were considered, one with a vertically oriented finned coil and one with a horizontal finned coil. Figure 1 shows schematics of the two configurations. There are two loops in the system, hot and cold, which alternately circulate nitrogen to heat or cool the packed bed. Each loop has a butterfly valve. The valve in the circulating loop is open and the valve in the idle loop is closed. These valves open and shut when the packed bed in the coil reaches the high and low temperature limits, switching operation from one loop to the other. The section with the packed bed is common to both loops. There is an electrical heater and a liquid nitrogen cooler in each loop to induce circulation. The flow is clockwise in both loops of the device with the vertically oriented finned coil and counter-clockwise in the device with the horizontally oriented finned coil.

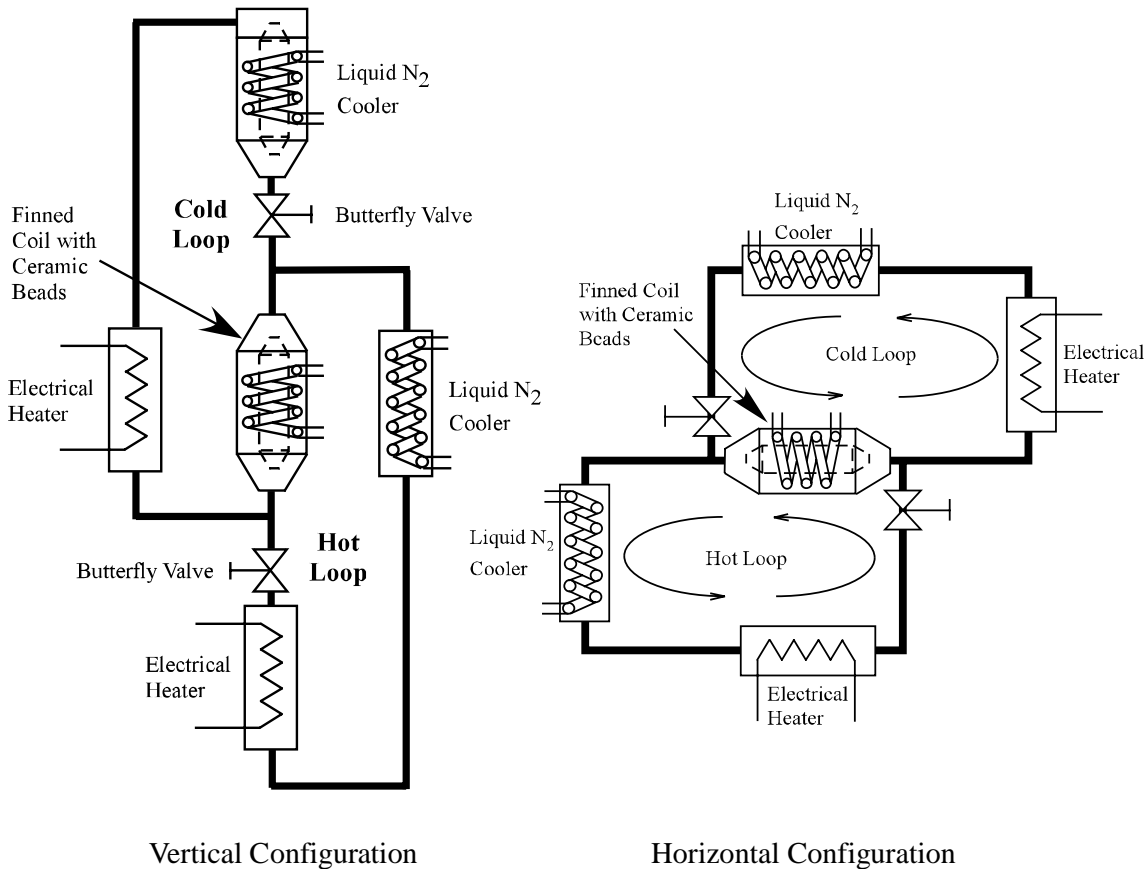


Fig. 1: Schematics of the two configurations of the double thermosyphon modelled.

Model Description

The hot and cold loops are modelled separately with one-dimensional momentum and thermal energy equations. The thermal inertia of the solid structures in the loops significantly impacts the heat-up and cool-down rates of the circulating nitrogen gas and therefore the packed bed. The solid structures in the sections are modelled with separate thermal energy equations, which are coupled to the fluid thermal energy equations through convection heat transfer. The boundary conditions for each loop are the specified surface temperature of the liquid nitrogen cooler and the electrical heater power.

The model alternately simulates circulation in the hot and cold loops. Flow in the hot loop is simulated until the packed bed reaches the upper temperature limit, at which time the model starts to simulate flow in the cold loop. The cold loop flow is simulated until the packed bed reaches the lower temperature limit,

and the pattern is repeated for a specified number of cycles. After ten cycles, the influence of the initial conditions is negligible and the flow is thereafter periodic.

Each loop is divided into six sections, for which momentum and thermal energy equations are developed. Figure 2 shows the segmentation of the hot and cold loops of the double thermosyphon with the horizontally oriented packed bed. Each loop of the vertical configuration double thermosyphon is similarly segmented. Section #5, containing the finned coil with the packed bed, is common to both loops. The sections in each loop, except for the one with the liquid nitrogen cooler, have solid heat structures with separate thermal energy equations. Since surface temperature of the nitrogen cooler is specified and the finned surface of the cooling coil has a much greater area than the housing, the thermal influence of the housing on the gas temperature is neglected. Section #5 has two heat structures. The finned coil containing the packed bed is one heat structure and the center insert and the steel housing is the other. The purpose of this model is to determine the transient temperature of the packed bed. The steel housing has most of the solid mass of section #5, and the coil has most of the surface area. It is therefore reasonable to expect the transient temperature responses of these two heat structures to differ significantly. Each loop has six heat structures, two of which are common to both loops.

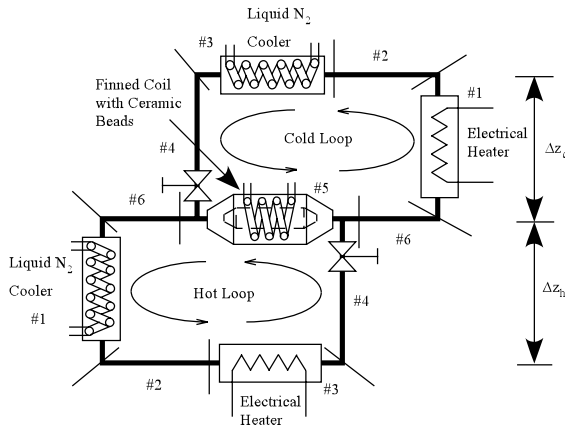


Fig. 2: Schematics showing the segmentation of the hot and cold loops.

Model Equations

The flow of the nitrogen gas is assumed to be incompressible, with the Boussinesq approximation that density is a linear function of temperature in the momentum equation body force terms.

$$\rho = \rho_0 [1 - \beta(T - T_0)] \quad (1)$$

The linear momentum equation, equation 2, is applied to each of the sections:

$$\frac{d}{dt} (m\bar{V}) + \dot{m}(\bar{V}_{out} - \bar{V}_{in}) = \sum \bar{F} \quad (2)$$

The loop flow area is assumed to be constant for the pressure and body force terms. This allows the six momentum equations can be added to obtain a single equation for the loop circulation flowrate. The actual flow areas are used to determine the irreversible loss terms. This assumption considerably simplifies the momentum equation, and it is reasonable for the low flowrates of natural circulation. Equation 3 is the finite-difference form of the momentum equation for the hot loop. With the fluid temperatures specified, this is a quadratic equation for the updated mass flowrate (\dot{m}^{n+1}) and it can be solved directly. The fluid temperatures are the averages of the previous and updated values.

$$\begin{aligned}
 & \left[\sum_{i=1}^6 L_i \right] \frac{\dot{m}^{n+1} - \dot{m}^n}{\Delta t} = \\
 & \rho_0 [1 - \beta(\bar{T}_1 - T_0)] A_f L_1 g - \\
 & \rho_0 [1 - \beta(\bar{T}_4 - T_0)] A_f L_4 g - \\
 & \frac{(\dot{m}^{n+1})^2 + 2\dot{m}^n \dot{m}^{n+1} + (\dot{m}^n)^2}{8\rho_0} \times \\
 & \sum_{i=1}^6 \frac{1}{A_i} \left(K + \frac{fL}{D} \right)_i
 \end{aligned} \quad (3)$$

Thermal energy equations update the section fluid temperatures. The flow direction is assumed, and upwind differencing is used. Energy equations for the heat structures update the temperatures of the solid structures in the sections. The heat transfer between the solid walls and the fluid in a section is by forced convection:

$$\dot{Q}_i = h_i A_{s_i} (\bar{T}_{HS_i} - \bar{T}_i) \quad (4)$$

Equations 5 and 6 are respectively the finite-difference forms of the thermal energy equations for the fluid and heat structure of the i^{th} section. Some of the section energy equations deviate from these generic forms: the packed bed section has two heat structures, the liquid nitrogen cooler section does not have a heat structure, and the fluid energy equation for the electrical heater section has a source term. The energy equations constitute a set of twelve simultaneous linear equations.

$$\begin{aligned}
 & \frac{T_i^{n+1} - T_i^n}{\Delta t} = \frac{(hA_s)_i}{\rho_0 \bar{A}_i L_i C_p} \times \\
 & \left(\frac{T_{HS_i}^{n+1} + T_{HS_i}^n}{2} - \frac{T_i^{n+1} + T_i^n}{2} \right) + \\
 & \frac{\dot{m}}{\rho_0 \bar{A}_i L_i} \left(\frac{T_{i-1}^{n+1} + T_{i-1}^n}{2} - \frac{T_i^{n+1} + T_i^n}{2} \right)
 \end{aligned} \quad (5)$$

$$\begin{aligned}
 & \frac{T_{HS_i}^{n+1} - T_{HS_i}^n}{\Delta t} = - \frac{(hA_s)_i}{(mC_p)_{HS_i}} \times \\
 & \left(\frac{T_{HS_i}^{n+1} + T_{HS_i}^n}{2} - \frac{T_i^{n+1} + T_i^n}{2} \right)
 \end{aligned} \quad (6)$$

The heater powers deposited in the gas in both the hot and cold loops are controlled by gas temperature limits. When the gas temperature exceeds the limit, electrical power to the heater element is shut-off. The actual power deposited in the flow varies due to thermal capacitance of the heater element. Equation 7 is used to update the heater power deposited in the gas when there is electrical power applied to the heater elements. This is the case when the heater gas temperature is less than the upper limit. When the gas temperature exceeds the upper limit, electrical power to the heater elements is interrupted. The finite-difference expression for the heater power to the fluid when the electrical power is shut-off is specified by equation 8. The parameter “ α ” is a function of the heater element geometry and the convection heat transfer coefficient.

$$\dot{Q}^{n+1} = \dot{Q}_0 - (\dot{Q}_0 - \dot{Q}^n) e^{-\alpha \Delta t} \quad (7)$$

$$\dot{Q}^{n+1} = \dot{Q}^n e^{-\alpha \Delta t} \quad (8)$$

Forced convection correlations for the Nusselt numbers and friction factors, as functions of the Reynolds number, are used. The average hydraulic diameter and flow area for a section are used to determine the Reynolds number. Irreversible loss coefficients account for elbows, expansions and contractions.

The solution procedure for a time step is to first assume values for the updated fluid temperatures and solve the momentum equation for the updated mass flowrate. The twelve energy equations are then solved simultaneously for the updated fluid and heat structure temperatures. The updated fluid temperatures are then substituted back into the momentum equation and a second iteration begins. The iterative process is repeated until values for the temperatures and mass flowrate converge. At this point the model advances to the next time step.

It is important to model the heat transfer in the idle loop, because the final temperature distribution in the loop, prior to the switch in circulating loops, provides initial conditions for the new circulating loop. The gas and the solid heat structure temperatures in the idle loop will tend to equilibrate due to heat transfer. There is no net flow through the idle loop, but gas in some adjacent sections will mix, and some stratification will also take place. The gas in sections that mix is assumed to be well mixed and is treated as a single lumped parameter. The solid heat structures are treated separately.

Results and Discussion

The double thermosyphon with the vertical configuration shown in figure 1 was initially modelled. The pipes have an inside diameter of 0.078 m, and the total height of the device is 2.737 m. A more compact design was desired, and this resulted in the horizontal configuration. The pipe diameter is the same for the second design, and the total height is a varied parameter. The loop control parameters are the same for both configurations. For the comparison between the performances of the two loops, the elevation changes in horizontal configuration loops are 0.635 m for both the hot and cold loops. The upper and lower temperature limits for the bead filled coil are respectively 423.0 K and 233.0 K. These are the temperatures at which operation switches from one loop to the other. The rated power of the hot loop heater is 6000.0 W and the gas temperature limit is 573.0 K. The rated power of the cold loop heater is 3000.0 W and the gas temperature limit is 283.0 K. When the gas temperature exceeds the limit, electrical power to the heater is terminated. The surface temperatures of the hot and cold loop liquid nitrogen chillers are respectively 283.0 K and 100.0 K.

Figures 3 and 4 show the transient coil temperatures and loop flowrates, with a pressure of 5.0 atm. (506.6 KPa), for single heating and cooling cycles of both thermosyphon configurations. As one might expect, the performance is degraded by reducing the elevation changes in the hot and cold loops. Both the heating and cooling phases of a cycle are slower with the horizontal configuration than with the vertical configuration. When operation switches from the hot to the cold loop, the cold loop heater does not turn on until the packed bed coil cools below the heater gas temperature limit. This delay is approximately six minutes for the vertical configuration and approximately twelve minutes for the horizontal configuration. Because the coil structure is oriented vertically with down-flow in the vertical configuration, the cold loop flowrate increases as the coil cools. The coil structure is oriented horizontally in the horizontal loop configuration, so the cold loop flowrate decreases as the coil cools. The buoyancy of the hot gas leaving section #5 provides the motive force for the cold loop until the heater starts to operate. Figures 5 and 6 show the transient coil temperatures and loop flowrates with a pressure of 10.0 atm. (1.013 MPa), and figures 7 and 8 show the transient coil temperatures and loop flowrates with a pressure of 15.0 atm. (1.52 MPa), for single heating and cooling cycles of both thermosyphon configurations. There is an increase in the cycle time for the vertical configuration between 10.0 and 15.0 atm. This is due to the increased heat up time. The heater deposited power is 6000.0 W for most of the time in both cases, and because of the higher mass flowrate

due to the higher density at the higher pressure, the gas temperature leaving the heater is lower at the higher pressure and the packed bed heats slower.

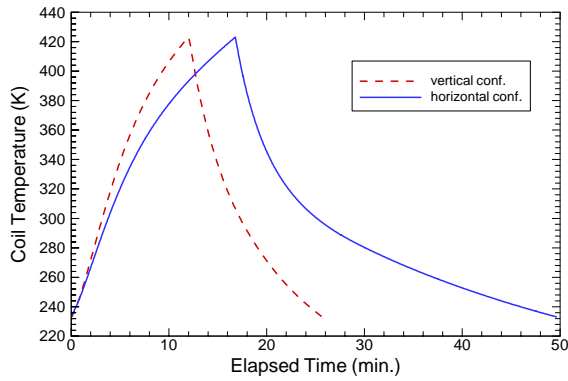


Fig. 3: Transient temperatures, for a single hot/cold loop cycle, of the packed beds in both vertical and horizontal configurations of the double thermosyphon. The reference pressure is 5.0 atm. (506.6 KPa).

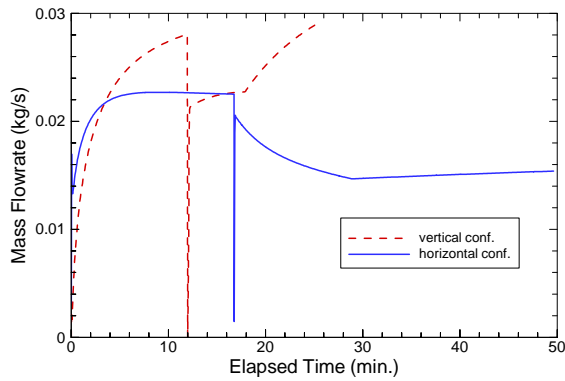


Fig. 4: Transient mass flowrates for a single hot/cold loop cycle of both vertical and horizontal configurations of the double thermosyphon. The reference pressure is 5.0 atm. (506.6 KPa).

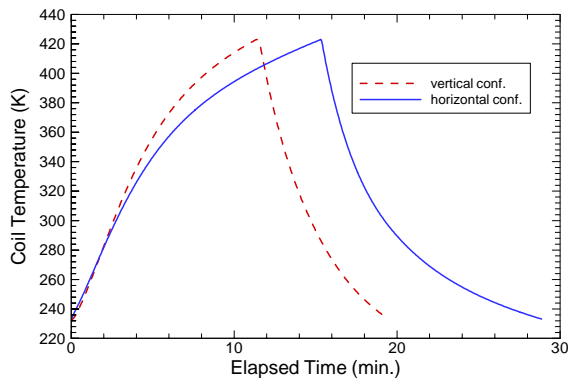


Fig. 5: Transient temperatures, for a single hot/cold loop cycle, of the packed beds in both vertical and horizontal configurations of the double thermosyphon. The reference pressure is 10.0 atm. (1.013 MPa).

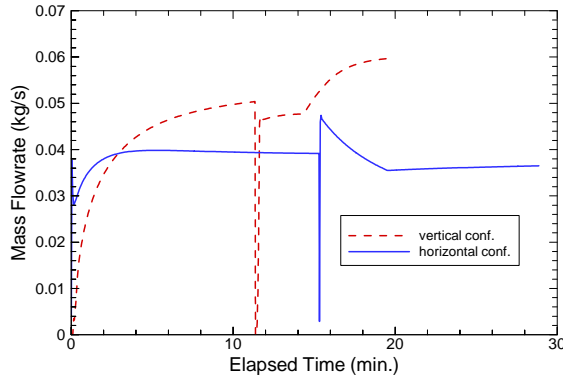


Fig. 6: Transient mass flowrates for a single hot/cold loop cycle of both vertical and horizontal configurations of the double thermosyphon. The reference pressure is 10.0 atm. (1.013 MPa).

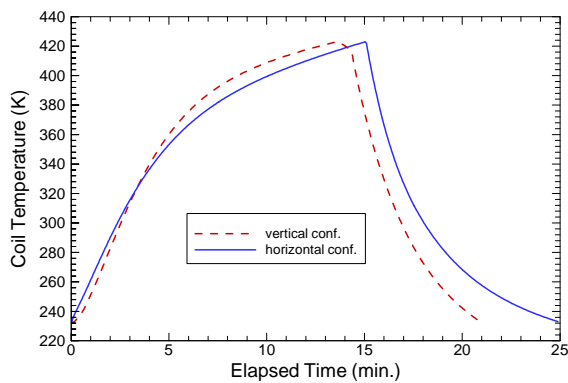


Fig. 7: Transient temperatures, for a single hot/cold loop cycle, of the packed beds in both vertical and horizontal configurations of the double thermosyphon. The reference pressure is 15.0 atm. (1.52 MPa).

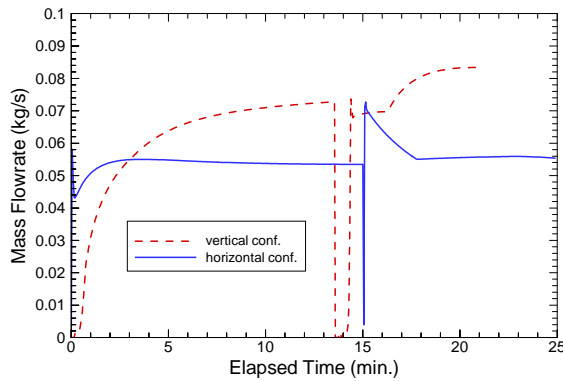


Fig. 8: Transient mass flowrates for a single hot/cold loop cycle of both vertical and horizontal configurations of the double thermosyphon. The reference pressure is 15.0 atm. (1.52 MPa).

Figures 9 and 10 show the packed bed temperatures and flowrates for a single hot/cold loop cycle for the horizontal configuration of the thermosyphon. The reference pressure is 10.0 atm (1.013 MPa) and results are shown for three different values of the total height ($\Delta z_h + \Delta z_c$). As the height increases, the heat up time of the packed increases because of the increasing mass of the heat structure as section #4 gets longer. This decreases the temperature of the gas entering section #5.

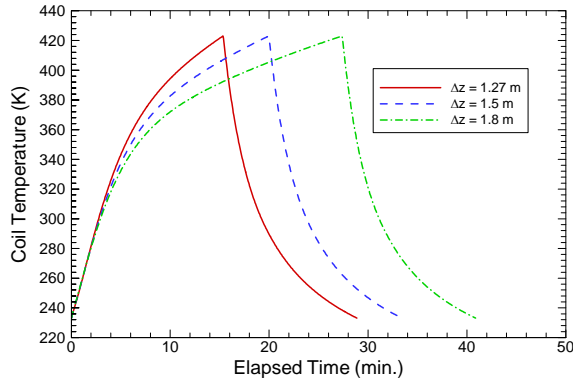


Fig. 9: Transient temperatures, for a single hot/cold loop cycle, of the packed bed in the horizontal configuration of the double thermosyphon. Results for three different total heights are shown. The reference pressure is 10.0 atm. (1.013 MPa).

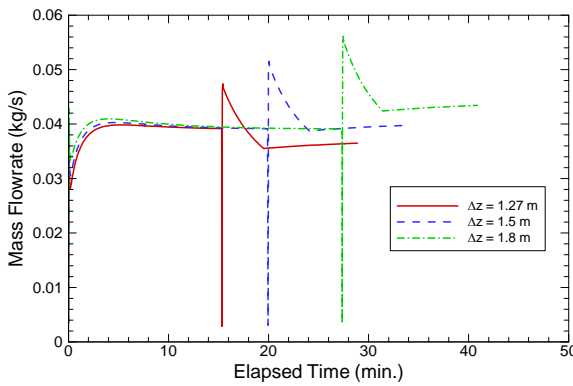


Fig. 10: Transient mass flowrates, for a single hot/cold loop cycle, of the packed bed in the horizontal configuration of the double thermosyphon. Results for three different total heights are shown. The reference pressure is 10.0 atm. (1.013 MPa)

Figures 11 and 12 show the transient hot loop section gas temperatures and heat structure temperatures for the horizontal configuration of the thermosyphon. The reference pressure is 10.0 atm (1.013 MPa) and the total height is 1.27 m. The gas temperatures for sections #2, 4, and 6 are not shown because they are essentially the same as sections #1, 3, and 5 respectively. These are sections with insulated pipe down stream of sections in which significant heat transfer occurs. Heat structure #5 is the steel housing of the finned coil and packed bed. The transient temperature of the packed bed is shown in fig. 5. The change in temperature of the packed bed is much greater than that of the housing.

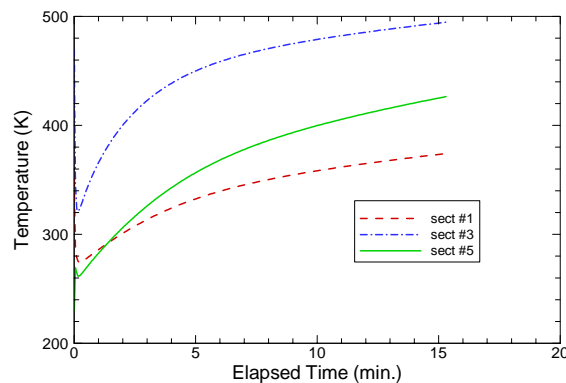


Fig. 11: Transient hot loop gas temperatures of the horizontal configuration. The reference pressure is 10.0 atm. (1.013 MPa) and the total height is 1.27 m.

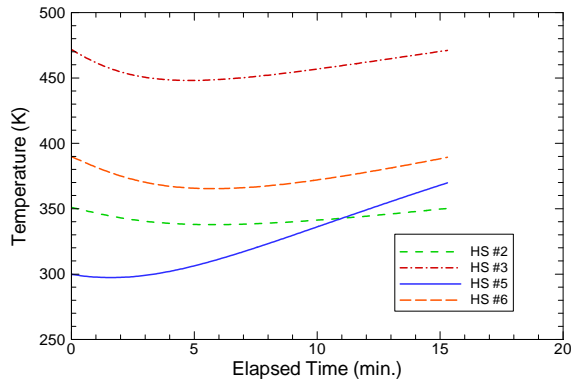


Fig. 12: Transient hot loop heat structure temperatures of the horizontal configuration. The reference pressure is 10.0 atm. (1.013 MPa) and the total height is 1.27 m.

Figure 13 shows the heater deposited power and gas temperature for a single hot/cold loop cycle for the horizontal configuration of the thermosyphon. The reference pressure is 10.0 atm (1.013 MPa) and the total height is 1.27 m. The heater in the hot loop is depositing the rated output of 6.0 KW into the gas for most of the transient. For the first four minutes of the cold loop portion of the cycle, the heater is off while the gas leaving section #5 drops to the upper temperature limit for the heater. Figure 6 shows the gas mass flowrate for this case.

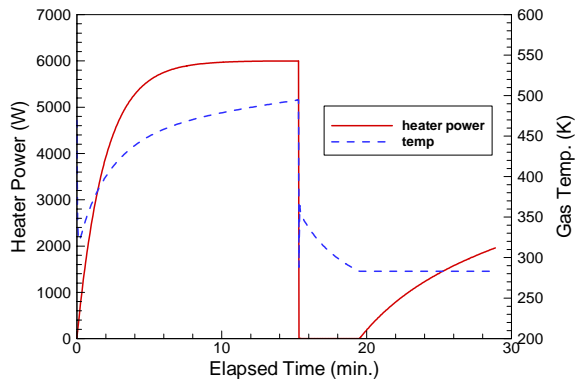


Fig. 13: Transient hot loop heater power and gas temperature of the horizontal configuration. The reference pressure is 10.0 atm. (1.013 MPa) and the total height is 1.27 m.

Conclusions

A one-dimensional transient model of the double thermosyphon has been developed. The model predicts the thermal response of a finned copper coil that is filled with palladium coated beads, as it is alternately heated and cooled by the natural circulation of nitrogen. This model was developed as a design aid for the double thermosyphon.